Study of the LHO 4K Recycling Cavity Sideband and Carrier Response to Excitation and Perturbations

G.D. Meadors[1], H.R. Gustafson[2]

[1]*Reed College*

[2]*University of Michigan*

The response of the LIGO Hanford Observatory 4-Kilometer Interferometer Recycling Cavity to perturbations is studied in this report, as observed when the Recycling Mirror is driven in length. Preliminary observations of power-recycling Michelson interferometry show the sideband amplitudes to respond oppositely while carrier amplitude remains roughly constant. This suggests that the Recycling Cavity length is not perfectly matched to input sideband light. Because the sidebands provide a reference system for detecting gravitational waves, it has been suggested that improving the match would improve LHO performance.

An optical heterodyning analysis system for the LHO 4-Kilometer Interferometer Recycling Cavity (pioneered by SURF students Evan Goetz and Richard Garrelts) has been re-engineered to yield a well-defined bandwidth and calibrated to the 1-2% level. In this system, carrier and sideband light from the Recycling Cavity is combined (beat) on a radiofrequency photodiode with a frequency shifted (75 MHz) reference beam fiber transported from the PSL laser system, yielding radiofrequency signals representing the higher sideband (at 50 MHz), carrier (75 MHz), and lower sideband (100 MHz). Demodulation electronics yields DC Root-Mean-Square amplitude signals for the LHO Data Acquisition system.

Background

The Laser Interferometer Gravitational Wave Observatory (LIGO) attempts to detect gravitational waves using three of the most precise surveying tools in the world: power-recycled Michelson interferometers with Fabry-Perot arms. Each of these interferometers has many parts that must cooperate to quiet noise, to make fine observations, and to gain a chance to listen to the stars. For the past two years at the LIGO Hanford Observatory (LHO), efforts have been underway to test the tuning of the power-recycling cavity of a four-kilometer interferometer. Real tests began this summer–and the gates to further mysteries have been opened.

Understanding the problems possible at the core of the LHO 4K interferometer (IFO) requires understanding the operation of the interferometers. Each L-shaped IFO contains components in three main sections [1]. A 1064 nm Nd:YAG pre-stabilized laser (PSL) and its frequency-stabilization system (FSS), a pre-mode cleaner (PMC), three electro-optic modulators (EOM's), and an input-mode cleaner (IMC) provide light input to the IFO. A recycling mirror (RM), beam splitter (BS), two input test masses (ITM's) and two end test masses (ETM's) form optical cavities to sensitize light to gravitational waves–these components are the body of the IFO. Five radio frequency photodiodes (RFPD's) detect the IFO's output.

In this "Initial LIGO" configuration, a laser beam enters the IFO, can pass through the RM, is incident upon the BS, and splits into two optical paths, one for each arm of the L. The arms are labeled 'X' and 'Y', analogously to the basis vectors of the Cartesian plane, and have corresponding ITMX and ITMY along with ETMX and ETMY. Along each optical path, the beam passes

through an ITM and enters into a Fabry-Perot (FP) cavity between that arm's ITM and ETM. In this cavity the beam resonates, exiting through the ITM after around a hundred round trips. Both X and Y optical paths rejoin at the BS, as in any Michelson interferometer. Half of the resulting beam is sent toward the output RFPD's through the "antisymmetric (AS) port," also known as the "dark port," whereas the other half is sent through the "bright port," toward the RM, reflected, and repeats the process of the input beam[2], except with reduced intensity and increased scatter and noise. In the absence of a gravitational wave, Michelson interference is destructive at the dark port and the amplitude of the light incident on the AS RFPD's is null; bright port interference is constructive. Gravitational waves are detected through LIGO's feedback systems, which reveal when the light on the AS RFPD's would not be null. the Initial LIGO configuration is diagrammed in Figure 1.

The subject of this study, the recycling cavity (RC), is a T-shaped optical cavity in medium-quality vacuum. Extending from the RM through the BS to both ITMX and ITMY, the one-way optical path length is estimated to be 9.38 m. This figure is derived from as-built construction schematics and is between the reflective coatings of the RM and ITMX, and is assumed (unless noted otherwise) to be the same to the millimeter scale for both paths. This assumption, together with the 50:50 ratio of the BS, permits the analysis of the RC as a 'simple' single FP cavity formed between the RM and a virtual 'average' test mass. Simplification of RC is used to justify the derivation of the error signal used to control RC length [1]. LIGO Livingston Observatory tests have nevertheless shown that unexpectedly large changes in beam shape can occur even with nanometer-scale changes in cavity length [3]; hence, treating the RC as a simple FP might not be a valid assumption for this study.

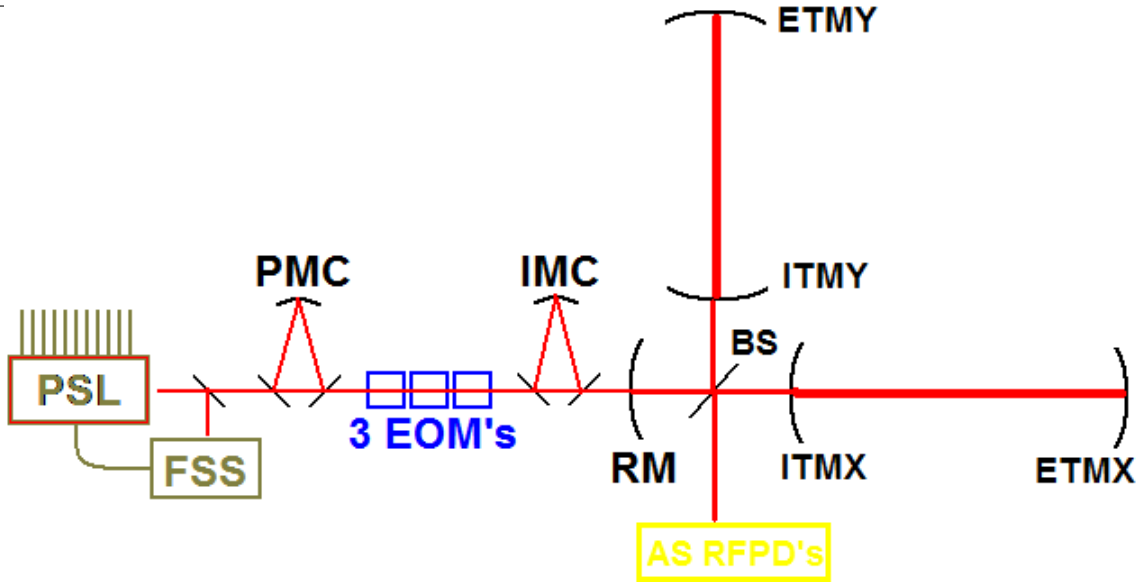

Figure 1: *Initial LIGO Configuration–primary optical components of a 4-kilometer interferometer are displayed. The RC is a compound Fabry-Perot cavity formed between the RM and ITM's X and Y. In high quality locking, carrier laser frequency is adjusted to maintain resonance in the RC. During excitation, the RM is moved sinusoidally on the micrometer scale, on the order of the laser wavelength.*

LIGO employs RC's for at least two purposes: increasing the power of the laser beam used to detect gravitational waves (GW), which decreases shot noise due to the quantum nature of light [4], and containing a reference for determining when GW are detected. Increasing light power is straightforward: without an RM, light returning from the FP cavity arms and not directed toward the AS RFPD's would be lost. With an RM, the light from the bright port–which is almost as bright as the input laser light in the absence of a gravitational wave–can reenter the IFO system up to about thirty times. This increases the effective power of the laser beam.

Providing the reference for GW detection proves more elaborate. Recall the EOM's in the input stage of the IFO. Each EOM, in series, applies phase modulation (PM) to the laser beam that passes through it. Oscillating at 24.48 MHz, 33 MHz, and 62 MHz, each device can add or subtract up to about a radian of phase from that laser light. PM is nearly equivalent to the introduction of two sideband frequencies–light at the carrier frequency plus and minus the frequency of the EOM. Only the sidebands at about plus and minus 24.48 MHz enter the main IFO. The former sideband is known as the higher (HSB) and the latter is called the lower (LSB).

Via what is called locking, the sidebands can be used to make the FP cavities in the arms resonate [5], by using the Pound-Drever-Hall (PDH) technique. Assuming that the arms are locked, the sidebands also provide the aforementioned reference for GW detection. Demodulation of the AS RFPD signals at 24.48 MHz can reveal how the carrier has changed with respect to the HSB and LSB [4]. The RC must be well tuned to allow this scheme. Note that if the sidebands were to enter the FP arms just as the carrier did, no relative phase change could occur. Because Fabry-Perot cavities reflect light far from their resonant frequencies, adjusting the sidebands to frequencies non-resonant frequencies for the arms traps the sidebands in the RC. Because the RC itself behaves as an FP cavity, the HSB and LSB must resonate there to reach the AS RFPD's.

To provide a consistent reference, both the HSB and LSB phases within the RC must either stay constant or vary oppositely so as to produce no net relative phase change with respect to the carrier.

Until this project was developed, no way existed to track the behavior of the HSB and LSB in

the RC. Sideband phase is especially difficult to observe, as the layout of light pickoffs (PO's) from the RC implies that any reference light with which the sidebands could be compared would have to travel over optical fiber. Unfortunately, optical fiber is highly sensitive to phase noise, so phase observation must be rejected for the time being. Yet this project has been able to observe HSB and LSB amplitude in the RC, as well as the amplitude of the carrier and the 2f beat frequency between the sidebands.

Amplitude can also give clues about how well the RC is tuned for resonance for the carrier, HSB, and LSB. This project has attempted to directly observe the relative response of both sidebands and the carrier in the RC when cavity length varies. Varying, or exciting, the recycling cavity length was performed by pushing the RM using its attached magnetic drivers (used to maintain low) at low frequency and amplitude. By taking data on the carrier and sideband relative amplitudes during this excitation and comparing the induced oscillation in their amplitudes to the excitation, it is possible to observe how close the sidebands are to resonance. If both HSB and LSB were perfectly resonate, then changes in cavity length would cause the sidebands amplitude to fall simultaneously. If either sideband were off-resonance, sideband amplitude oscillations could occur out-of-phase, dependent on the distance of the sidebands from resonance.

Findings

For reference to the figures, the following Table 1 provides the correspondences between the observed frequencies and their data channels:

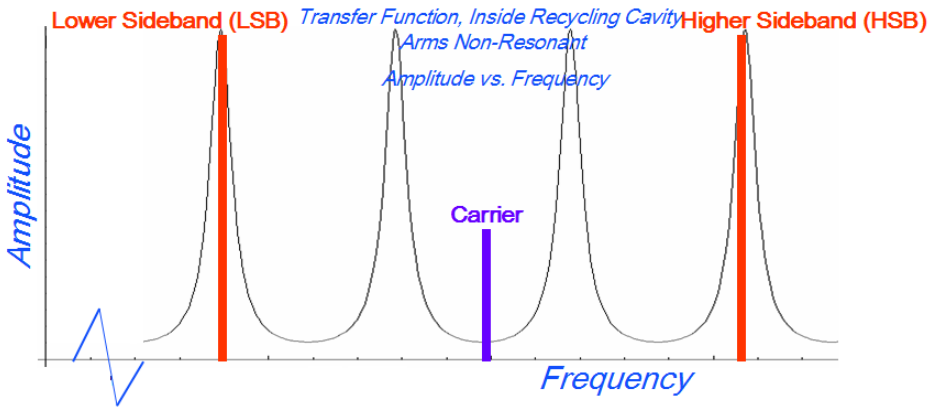

Figure 2: *Fabry-Perot resonant gain in amplitude versus frequency. In color, the sidebands and carrier are plotted. The carrier is displayed at an anti-resonant point, although when the arms are including, the mirror's reflectivity changes for the carrier such that the carrier becomes resonant as well. Note that changes in cavity length, as well as adjustments of carrier laser frequency, change the relative position of the black graph with respect to the colored sidebands and carrier.*

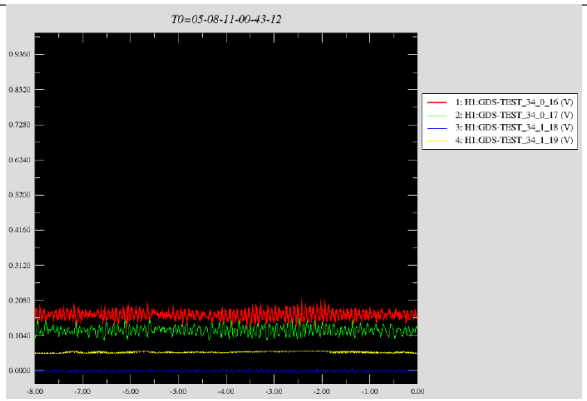

Figure 3: *LHO in very low-quality lock, unexcited. This time series includes the HSB (red), LSB (green), 2f (blue), and Carrier (yellow). Notice that a bounce mode for the interferometer ITM's is still visible at about 12 Hz, and that the HSB and LSB response is about 180 degrees out-of-phase. Further notice the discrepancy in sideband amplitudes in spite of much calibration–it would appear that the sidebands have unequal resonant gain inside the RC. CAUTION: for this and following figures, different gain factors apply to the carrier, compared to the HSB & LSB, compared to the 2f.*

LHO has been observed in many states using the recycling cavity analyzer, although few of these observations yet suggestion specific understandable phenomena. Time series of the RC are somewhat revealing, as in Figures 3 and 4, displaying noticeable bounce modes [6] at 12 that affect HSB and LSB but not 2f or Carrier. In the RC, the cause of the the 12 Hz mode is probably due mainly to the ITMX and ITMY vertical pendulum modes and perhaps partly from the RM and BS vertical pendulum modes [7]. Power spectra reveal another effect in the carrier, at 17 Hz; the effect is likely due to the ITMX optical lever effect, although the BS pendulum roll mode at 18.5 Hz could

Table 1: Optical frequencies observed via digital data channels

Optical frequency	Data Channel
HSB	H1(fast): GDS-TEST_34_0_16
LSB	H1(fast): GDS-TEST_34_0_17
2f	H1(fast): GDS-TEST_34_1_18
Carrier	H1(fast): GDS-TEST_34_1_19

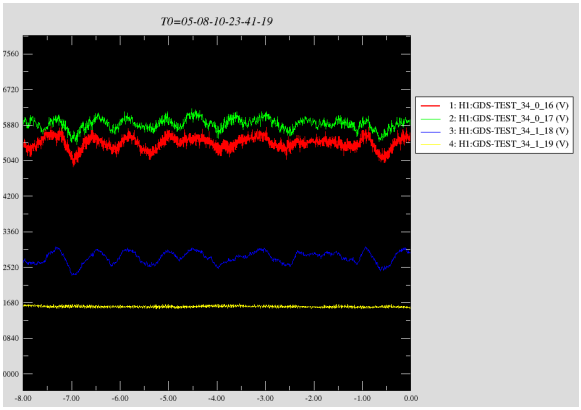

Figure 4: *LHO in high-quality lock, unexcited, with Power Recycling Michelson (PRM) from the RM to the ITM's as well as FP arms locked. 12 Hz bounce mode [6] is less obvious but present; LSB and HSB response appears to be still out-of-phase. 2f (technically the product of HSB and LSB) tracks the LSB and HSB, and does not show the 12 Hz mode. In this time series, the relatively constancy of the Carrier is in contrast to the sidebands' variations. The sidebands have dramatic low-frequency noise that affects HSB and LSB mostly in-phase. LSB is noticeably larger than HSB.*

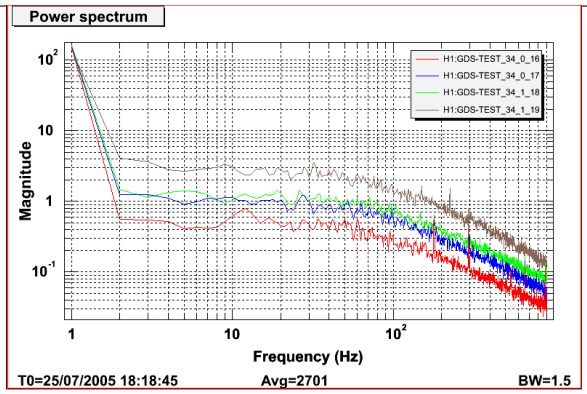

Figure 5: *LHO in very low-quality lock, unexcited. This power spectrum (FFT) of the HSB (red), LSB (blue), 2f (yellow), and Carrier (brown) displays a typical noise baseline for the recycling cavity analyzer. Notice the 1/f frequency roll-off with the -3dB point occurring around 110 Hz, due to the averaging circuit in the electronic demodulator. Significantly noise is visible around 120 Hz. Due to bin width, noise appears very high below 1 Hz.*

play a part. The prominent 55 Hz noise on Figures 6 and 7 is most likely related to the reference fiber used to extract the HSB, LSB, and Carrier signals, since it is not seen on the 2f spectrum. Noise sources documented at 55 Hz include the Laser Vacuum Equipment Area (LVEA, where LIGO optical components are established) chiller pad water and air compressors. As the sidebands are introduced before light enters the RC, it is unclear why the 12 Hz feature only appears on the sidebands and the 17 Hz feature only on the carrier, but it is sensible that compressor noise would affect the optical reference fiber. Note that none of these features are visible in Figure 5, taken when the interferometer was out-of-lock.

The time series also display large low-frequency variation in the sidebands that does not occur in the carrier. Figure 4 shows this to great effect; it is not atypical for both the HSB and LSB

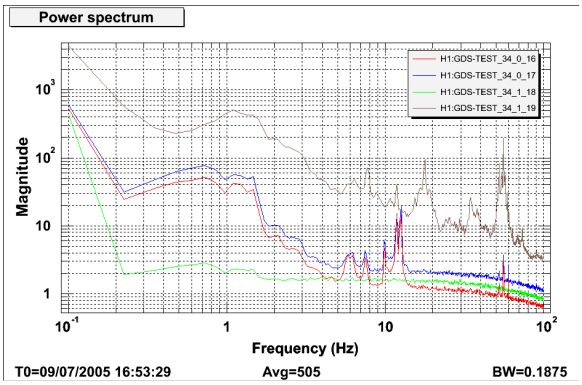

Figure 6: *LHO in lock, unexcited, but only in PRM configuration without FP arms. Substantial low-frequency noise affects all channels. Bounce modes are visible at 12 Hz in the LSB and HSB, 17 Hz in the Carrier. Theoretically, the Carrier should not even be detectable because the FP arms are not resonant. An undiagnosed noise source is present at 55 Hz for HSB, LSB, and Carrier, but not 2f–possibly due to the reference fiber described in the Methodology section. Otherwise, smooth roll-off occurs at high frequency.*

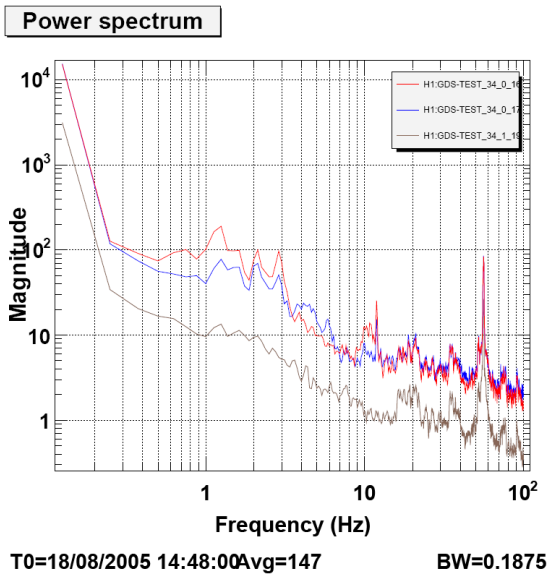

Figure 7: *LHO in lock, unexcited, with PRM and FP arms. Additional noise appears to have been introduced by the arms in the HSB, LSB, and carrier. 12 Hz and 17 Hz bounce modes are still present in the sidebands and carrier, respectively, and the 55 Hz noise source is present in both. As before, the LSB is slightly larger than the HSB at many frequencies. Smooth roll-off occurs beneath substantial noise.*

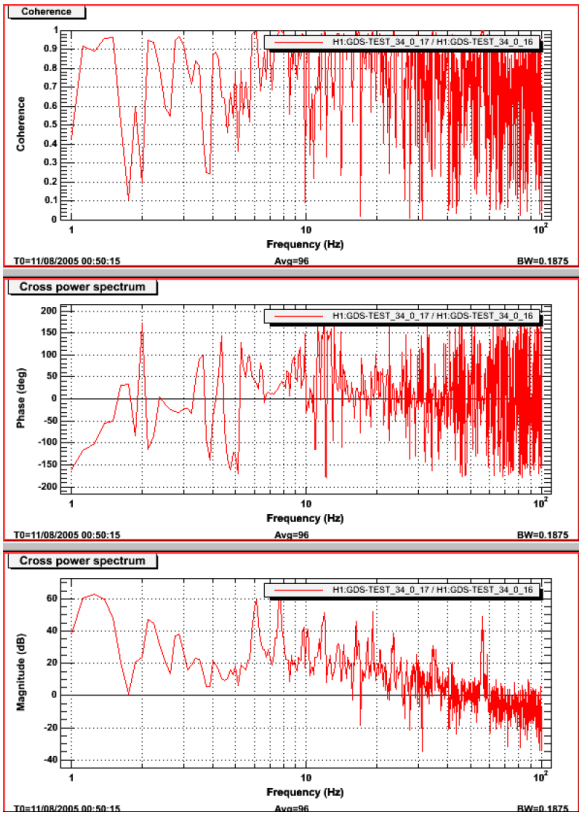

Figure 8: *LHO in lock, unexcited, with PRM and FP arms. This set of graphs compares the coherence, phase relationship and magnitude of the HSB and LSB from 1 to 100 Hz. Coherence is relatively high but drops at numerous frequencies. Phase difference (in the amplitude response) is centered around 0 degrees but fluctuates. Magnitude ratio is centered around 0 dB, but the LSB often has higher magnitude than the HSB, especially where the coherence value is high. Phase differences do not appear to be correlated. 96 averages. Taken on 10 August 2005*

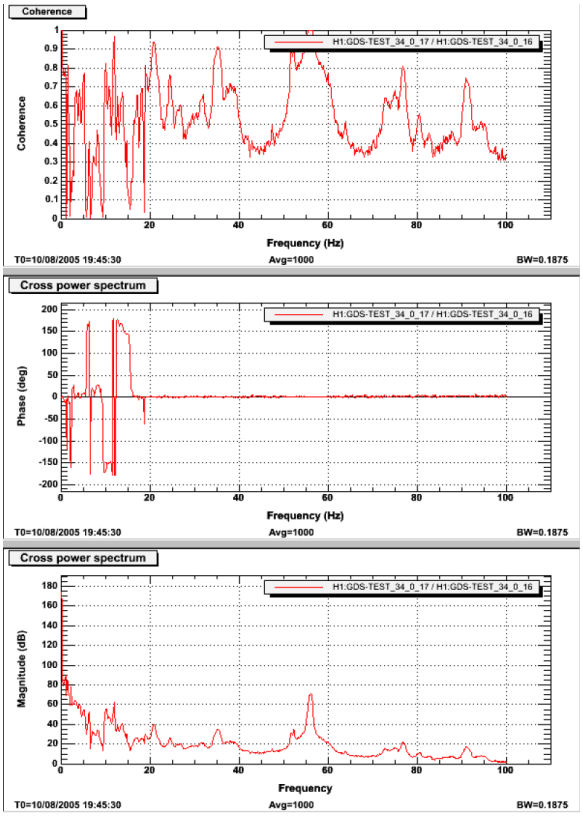

Figure 9: *LHO in high-quality lock, excited at 20 Hz, with PRM and FP arms. Excitation was at relatively low amplitude and may not have produced a measurable effect on this graph. The graph again compares the coherence, phase relationship and magnitude of the HSB and LSB. LSB was uniformly larger in magnitude, although the ratio decreases at high frequency. Peaks in the ratio are correlated with peaks in the coherence. Below 20 Hz, the phase response of he LSB and HSB differs significantly; about 20 Hz the sidebands appear to be nearly perfectly in-phase. 1000 averages. Taken on 10 August 2005.*

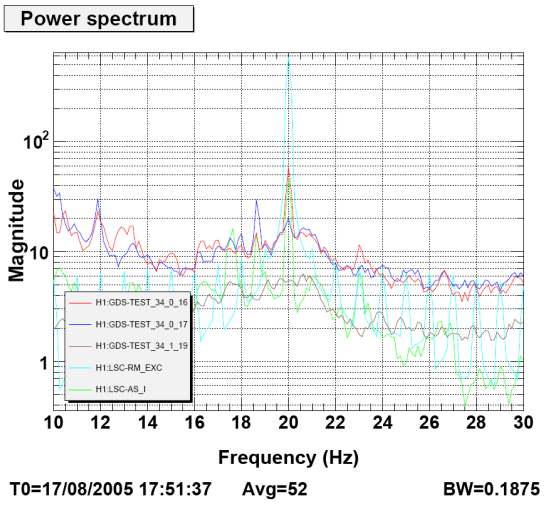

Figure 10: *LHO in high-quality lock, excited at 20 Hz, with PRM and FP arms. Power spectrum of the HSB, LSB, and Carrier response to a 20 Hz excitation (also graphed); antisymmetric in-phase (AS_I) light from the main LHO output is displayed. HSB responds strongly at 20 Hz, LSB weakly, Carrier hardly at all. AS_I likewise peaks at 20 Hz, indicating correlation with the disturbances in the sidebands due to the RM movement. Taken on 17 August 2005.*

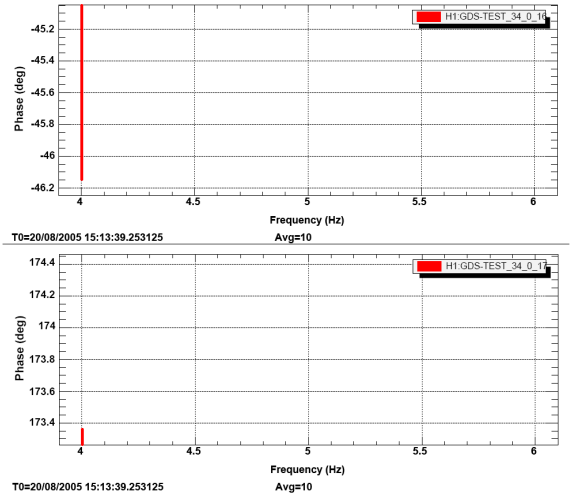

Figure 11: *LHO in high-quality lock, excited at 4 Hz, with PRM and FP arms. Phase relationship of the HSB compared to the excitation channel and the LSB compared to the excitation channel. The HSB appears to respond 220 degrees out of phase with the LSB, suggesting that the sidebands are located on opposite sides of resonant gain peaks (see Figure 2). Taken on 20 August 2005.*

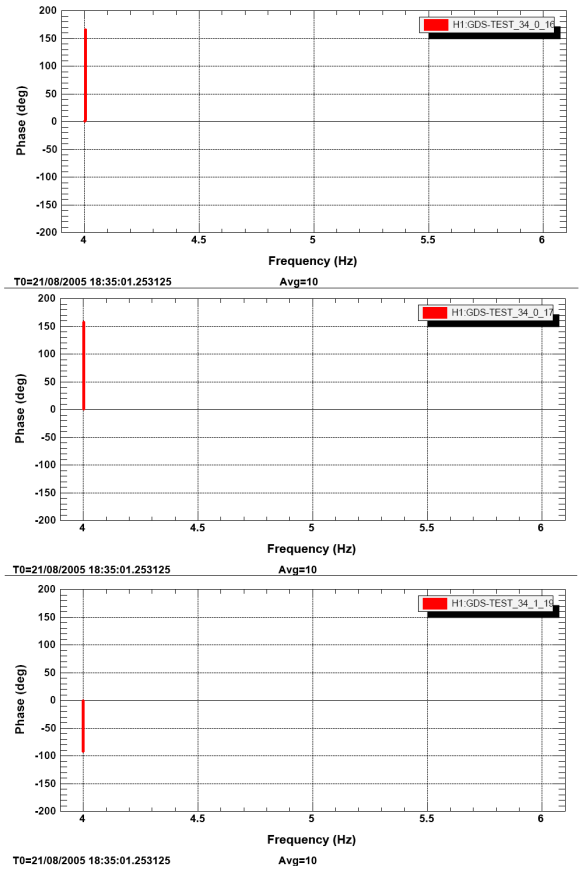

Figure 12: *LHO in high-quality lock, excited at 4 Hz, with PRM and FP arms. Phase relationship of the HSB compared to the excitation channel and the LSB compared to the excitation channel. The HSB appears to respond only 10 degrees out of phase with the LSB, suggesting that the sidebands are located on the same side (or, both at the top of) resonant gain peaks. However, the carrier responds about 260 degrees behind them both. This would imply that the carrier may be offset from its resonant peak, and, because the sidebands are dependent on the carrier, that the sidebands are at least occasionally also offset from their resonance peaks. This effect may be minor, but could explain the difference of this result from that of Figure 12. Taken 21 August 2005*

to drop in quasi-periodic patterns, roughly in phase, by factors of 20 percent or more. Roughly in-phase is key: as can be seen in Figure 9, the sidebands are often out-of-phase in response to these variations, even when 1000 averages of data are taken. Figure 8 also shows low coherence between the sidebands at all frequencies, but notably in the low-frequency region. There is substantial noise in this region, including HAM stack, BSC stack, and highway trucks [7], but it is initially unclear why any of these affects should cause amplitude changes in the HSB and LSB out-of-phase. These reason may be connected with the out-of-phase responses to excitations that was sometimes observed.

Excitations did prove to be a useful way of exploring the recycling cavity, and it is unfortunately that not more data was taken. It is evident from Figure 10 that there is at least a correlation between excitation of the RM, oscillation in sideband amplitude at 20 Hz, difference in sideband magnitudes, and a persistent index of noise–the in-phase signal from the asymmetric port of the BS, known as AS_I. AS_I is ideally null, and non-zero AS_I contributes shot noise to LIGO, limiting sensitivity above 150 Hz [1]. It is somewhat sensible that AS_I would be large at the excitation frequency; at least at the reflection port preceding the RM, AS_I is sensitive to changes in power recycling cavity length [1]. The control scheme for the recycling cavity depends on the assumption that reflection port light goes to zero; the failure of this control scheme at the excitation frequency could lead to the generation of AS_I elsewhere that passed the antisymmetric port and was read out.

The response of the HSB and LSB proved confounding. Foremost, it is frustrating that large,

unexplained variations occurred in the sidebands at low frequency and were not present in the carrier–the length control system for the RC relies on maintaining a constant ratio of the carrier to sideband gain [1]. On the other hand, the constancy of the carrier could be indicative that the length control system is working properly for the carrier. Why it cannot also work for the sidebands is uncertain; the optical levels of the sideband frequencies shift as much as the carrier whenever the PSL frequency is adjusted, as it is in "Common Mode" locking. This in principle should keep all three frequencies locked–if they are each near the top of their resonance peaks, depicted in Figure 2.

Results as shown in Figures 11 and 12 suggest that the HSB and LSB may not be at the top of their resonance peaks. On 20 August 2005, in Figure 11, the differing phase responses of the HSB and LSB to excitation–nearly 180 degrees apart, suggested that the cavity length was such that if the HSB was too high or low in frequency, the LSB was respectively too low or high. However, on 21 August, the HSB and LSB responded in-phase. The carrier was out of phase with both sidebands and the excitation frequency. This would suggest that HSB and LSB were (at any one time) both either too low or too high, due to the off-centering of the carrier. Under these conditions, when the carrier is locked, it is not possible for both HSB and LSB to be locked simultaneously (although either one could be locked by changing cavity length).

The off-centering of the carrier resonance point might explain the large variations in sideband amplitude despite carrier constancy. A resonant carrier would resultant in at least one non-resonant sideband; off resonance, the differential amplitude response of the sideband to changes in cavity

length would be significantly greater. This phenomenon could also be responsible for the different resonant gains of the HSB and LSB, although this phenomenon has been observed even when the interferometer is not resonant, as in Figure 3.

Carrier constancy could also be increased due to the damping effect of the arms. Light at the carrier frequency is resonant in both the FP arms and the RC; the sideband light is resonant in the RC, and so should most suffer the effects of RC deviation from resonance.

Discussion

More data needs to be taken so as to understand the relative contribution of the damping effects of the FP arms and the possible off-centering of the carrier resonance point in the RC.

Additional theoretical work should be done to explain how off-centering of the carrier from resonance could arise.

It is possible that the finite thickness of the reflective dielectric coating on the ITM's may be at fault for an off-center carrier. Prior work seems to assume that the coatings are infinitely thin, while still exploiting the fact that the carrier reflectivity off the arms is a resonant reflectivity determined by the carrier's resonance in the FP arms. Sideband reflectivity is determined by the Michelson asymmetry in the RC [1].The error signal for controlling RC cavity length, or instead PSL laser frequency at high stages of locking, is proportional to the sum of the carrier ITM reflectivity and the sidebands' ITM reflectivity. When the FP arms are locked, carrier reflectivity is constant and

negative. Sideband reflectivity is varied. However, it is only true that the sum of the reflectivities is useful if it can be assumed that making the carrier resonant in the arms and making the sidebands resonant in the RC in turn makes the carrier resonant in the RC. This is true only if the net phase change of the carrier transmitted through the dielectric mirror coating is a multiple of 360 degrees.

There is no reason to believe that the net phase change of the carrier transmitted through the dielectric mirror coating on the ITM's is a multiple of 360 degrees, unless manufacturing precautions were taken unbeknownst to the author or mentor of this paper. The carrier when resonant in the FP arm cavity has a constant zero electric field on the arm side of the mirror coating, but constant nonzero electric field on the RC side. This has the same phase effect as having the RC be the wrong length for the carrier, even if it is the right length for the sidebands. The black resonant peaks in Figure 2 would be shifted not quite halfway, from the carrier's perspective: off-centering would be produced. The locking system for the RC somehow seems to be able to re-center and resonate on the carrier, because of the remarkable stability of the carrier in Figures 3 and 4. The sidebands suffer: they are off-resonance, even if only slightly and (from the difference between Figures 11 and 12) perhaps by different amounts during different locking cycles. Off-resonance, they vary more, as seen in the figures. If cavity length is not properly 3/2 of the modulation frequency (as implied by Figure 2), then gain of the sidebands would also be different, as seen in all the time-series and power-spectra. The mirror coating hypothesis should be tested by future investigators.

Theoretical work also needs to be performed to discover the true significance of the deviation

of the sidebands from resonance, whatever the cause. If the sidebands were indeed off resonance and on the same side of resonance peaks due to an off-center carrier, then Pound-Drever-Hall correction for the FP arms could be hampered. The PDH technique relies on the relative phases of the sidebands and carrier in order to determine how to adjust FP cavity length or laser frequency so as to lock on the carrier [5]. An off-center carrier would produce a permanent phase offset between the carrier and sidebands, although this offset would be at DC and not directly compromise detection. It would instead limit the range of PDH locking.

Three additional points should be noted about off-resonance sidebands. Off-resonance sidebands are more phase stable that resonant sidebands, and could actually be useful for the purposes of locking the FP arms, though this would be counterproductive for demodulation of the AS port signal. Furthermore, the PDH error signal is linear for small carrier deviations from resonance in the FP arms [3] which ensures that small phase offsets of the sidebands with respect to the carrier do not produce supra-linear flaws in the error signal. Finally, the PDH scheme has been characterized, to first-order, to be unaffected by a constant non-zero relative phase difference of the reference (sideband) and driving (carrier) frequencies as well as fluctuations in sideband power well below the modulation frequency [5]. In the case of LIGO, if the off-centering theory is correct, then the non-zero phase difference between carrier and sidebands is normally constant–except when signal or noise is actually detected–and the modulation frequency of 24.480957 is well above the highest noise source for the 4K IFO [7]. These indicate that the phenomenon observed in this study were probably at worst second-order effects for LIGO.

Detection could be more affected than PDH control. The response of AS_Q and AS_I to failure of the sidebands to resonate perfectly in the RC should be investigated. It is known that the detection scheme assumes that the sidebands are perfectly anti-resonant in the FP arms [1]. If the carrier is properly centered on resonance in the FP arms, as is possible with working PDH, this should be true, but further study is warranted.

From this research and fact that LHO functions well in most other respects, it can be inferred that the RC is a reasonable length. The mirror coatings hypothesis implies that the carrier and sidebands see different cavity lengths, but this imperfections appear insignificant for FP arm length control–even if the in-cavity consequences, such as sideband amplitude variation, are dramatic. Detection, via the demodulation of the AS_Q signal, could be affected to a less well-known degree. However, it is clear that some substantial information about the nature of the RC can be detected from examining the sidebands, which was not possible before. Vibrational modes of the optics are visible, which could lead to in-cavity detection providing a supplementary noise control scheme.

Further into the future, it should be possible to transplant the recycling cavity analyzer in order to understand the mode cleaner. Like the RC, the MC must be resonant for sidebands and carrier. Experience in tuning the RC for resonant would carry over to the MC. Likewise, experience at the LIGO Hanford Observatory 4K IFO applies to the 2K as well as the 4K at Livingston. Better understanding of the nature of the LHO recycling cavity could help improve the noise performance of all LIGO recycling cavities. If the mirror coating hypothesis is true, then it may also reveal the differences in the ITM dielectric reflective coatings between the interferometers. Indeed, if

used in non-LIGO interferometers with different mirror manufacturers, then it could show what process yields the best coating thickness for use with 1064 nm Nd:YAG lasers. Through all these means, the recycling cavity analyzer will give valuable knowledge for future work in tuning the recycling cavities for Advanced LIGO and its successors, instruments scheduled to contain new signal recycling mirrors and still further mysteries.

Methods

Optical heterodyning. Laser light is sampled from Pickoff-Y (POY), which takes light reflected off of ITMY. A reference beam is also created using PSL light shifted upwards in frequency by 75.001000 MHz using an Isomet 1205C Acousto-Optic Modulator (AOM) [8]. The 75.001000 MHz frequency is currently produced by an HP ESG-1000A signal general and amplified by a ZHL-3A RF amplifier. This shifted reference beam is taken through fiber and brought back to space on optical table ISCT3, where it is heterodyned with the POY sample light through a beam-splitter. Half this light is incident on a beam dump, the other half is incident on a New Focus 1811 RFPD [6]. The New Focus 1811 RFPD has a 0.3 mm photodiode. A Thorlabs RFPD with a 1 mm photodiode was tested and the low frequency oscillations in the HSB channel were visually identical. This implies that the 0.3 mm is larger than the sampled beam width and is sufficient to accommodate beam jitter.

Light incident on the RFPD contains several carrier and sideband frequencies. The f-beat frequencies between both sidebands and the carrier exists at about 24.481957 MHz, and the 2f-beat frequency between the higher sideband (HSB) and lower sideband (LSB) exists at 48.962914

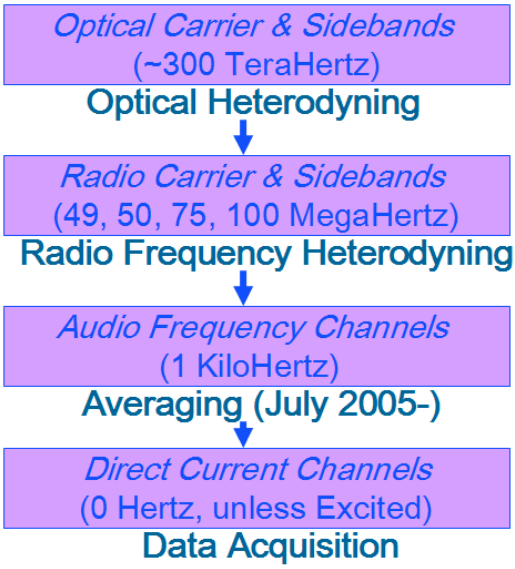

Figure 13: *Schematic of the carrier and sidebands analyzer for the recycling cavity. Four stages exist: laser light is sampled from Pickoff-Y (POY), heterodyned with a shifted reference beam and taken to an RFPD. The RFPD signal is then demodulated and reduced to audio frequency. The audio frequency is averaged, revealing only amplitude modulations that correspond to perturbations and excitations. This process attempts to circumvent problems with losing quadrature-phase information to the demodulation signal, at the expense of information about the optical phase relationship of the sidebands; this does not lose information about the phase of the amplitude response of the sidebands to excitation.*

MHz. The HSB is present at 50.520943 MHz, the Carrier at 75.001, and the LSB at 99.481957 MHz.

The New Focus 1811 RFPD is rated to have a -3 dB roll-off (single-pole) at 125 MHz. This was consistent with tests with an HSB-frequency signal and an LSB-frequency signal produced by the same Electro-Optical Modulator (EOM). RF frequencies were outputted by the RFPD with the HSB (around 50 MHz) being greater than the LSB (around 99.5 MHz) by a ratio of about 0.74 dB. This output is the same as that delivered to the electronic demodulating portion of the analyzer.

Electronic demodulating. Electronic demodulation of the RFPD signal occurs in two steps: RF heterodyning and audio frequency averaging. The RF heterodyning occurs when an amplified RFPD signal is sent into the RF ports of a set of four mixers. The LO ports of those mixers each receive one amongst a set of frequencies, generated locally by a combination of another HP ESG-1000A signal generator at 75.000000 MHz and a Stanford Research DS345 at 24.480957 MHz, that are 1 kHz offset from either the HSB, LSB, Carrier, or 2f. The IR ports of the mixers produce signals that are individually sent through appropriate bandpass filters, and then amplified using four Stanford Research 560 pre-amplifiers. The resultant signals separately contain amplitude and phase information for the HSB, LSB, Carrier and 2f, but are shifted down in frequency to 1 kHz.

Amplitude information is extracted (but phase information lost) when the four 1 kHz signals are each sent through an averaging circuit. This averaging circuit is made up of an Analog Devices 736JN chip coupled with two 330 nF PPS film capacitors. This circuit produces a DC output equivalent to the RMS value of the input, which only varies if the signal amplitude varies. The

AD736JN is well-documented [9] but is incapable of performing True RMS measurement; hence, the averaging circuit is most accurate for when the 1 kHz signals are sinusoidal. The output of the averaging circuit contains an inherent low-pass frequency effect due to the capacitors, with a single-pole -3 dB roll-off at about 110 Hz.

The outputs of the averaging circuits are sent through RC low-pass filters at about 300 Hz before being sent to four Data Acquisition (DAQ) channels. Each of these channels has input impedances of about 47 k Ω, much higher than the resistances of the filters. The DAQ channels are observable over the LHO computer network, and are as described in the Findings section.

Additional unattested attenuators have also been placed in the electronic demodulation system in order to make the values produced by the GDS test channels equal for equal amplitude light input to the RFPD, especially for the sidebands. The final difference between the GDS test channels has been measured as being as low as 0.12 dB, with the LSB being larger, although the measurement is complicated by issues of DC offset in the DAQ. However, the system is very capable of making measurements on the 0.5 dB level about th different in sideband amplitudes.

Excitations, perturbations and analysis. Excitation of the recycling mirror at low frequency allows the study of the response of the sidebands and carrier to changes in cavity length. The phase of the response with respect to the excitation narrows the possibilities regarding which side of resonance a given channel is on–the situation in Figure 2 can be empirically tested. Although measurements of the dynamic responses of the LIGO interferometers using high frequency excitation have been done before by Rakhmanov, Savage, Reitze and Tanner [10,11], those studies focused on

examining the 4 kilometer arms. This study tests the recycling cavity, which has not been done before in this way.

To excite the recycling mirror, the channel H1(slow): LSC-RM_EXC is driven with a sinusoidal wave, input using the computer program DTT. For this program, amplitude values of greater than 100 are appropriate. Large amplitudes are necessary to overcome the locking mechanism of the RC, described as having a unity gain frequency (single-pole) of 150 Hz [1]. As the electronic demodulation set had a lower cutoff frequency of 110 Hz, the using a large amplitude proved the best option. Offsets to the sine wave can also be applied. Frequencies of greater than 1 Hz should, in principle, be visible above the noise of the recycling cavity analyzer. A power spectrum of the GDS channels for the analyzer should reveal whether the excitation is having significant effect; typical LIGO perturbations may have comparable magnitude even with a high-amplitude excitation. Note; DTT is also capable of comparing the amplitude response of each channel to the excitation channel, revealing the magnitude, phase, and coherence of the sideband and carrier frequencies with respect to the excitation. See Figures 11 and 12 for examples.

1. Fritschel, P. *et al.* Readout and control of a power-recycled interferometric gravitational wave antenna. *Appl. Opt.* **40**, 4988 (2001).

2. Weiss, R. The LIGO interferometers: how they work and how well they work. Tech. Rep. G030024-00-D, Laser Interferometer Gravitational Wave Observatory (2003).

3. Gretarsson, A., Frolov, V., O'Reilly, B., D'Ambrosio, E. & Fritschel, P. Fields in the recycling cavity at the LIGO Livingston Observatory. Tech. Rep. T050040-00-D, Laser Interferometer

Gravitational Wave Observatory (2005).

4. Saulson, P. *Fundamentals of interferometric gravitational wave detectors* (World Scientific, Singapore, 1994).

5. Black, E. Notes on the Pound-Drever-Hall technique. Tech. Rep. T980045-00-D, Laser Interferometer Gravitational Wave Observatory (1998).

6. Gustafson, D. Analyzing system and reference beam for individually monitoring recycling cavity and carrier dynamics. Tech. Rep. T050004-00-I, Laser Interferometer Gravitational Wave Observatory (2005).

7. Berkowitz, R., Landry, M., Ottaway, D. & Schofield, R. Summary of mechanical resonances in the Hanford LIGO Interferometers. https://gold.ligo-wa.caltech.edu/ (2003). Online list on a secure LIGO server.

8. Gustafon, D. Sideband and carrier analyzer system (2005). Unpublished.

9. Analog Devices, Norwood, MA. *AD736: Low cost, low power, true RMS-to-DC converter* (2005).

10. Rakhmanov, M., Savage, R. J., Reitze, D. & Tanner, D. Dynamic resonance of light in Fabry-Perot cavities. Tech. Rep. P010013-00-D, Laser Interferometer Gravitational Wave Observatory (2001).

11. Rakhmanov, M. & Savage, R. Measurement of dynamic responses of the 4-km LIGO Fabry-Perot arm cavities. Tech. Rep. G040045-00-Z, Laser Interferometer Gravitational Wave Observatory (2004).

Acknowledgments To Dr. H. Richard (Dick) Gustafson, mentor for this project and dedicated Recycling Cavity tuner for at least the past two years; To Evan Goetz and Richard Garrelts, for their hard work designing and building the instruments used herein; To Dr. Keita Kawabe, Dr. Rick Savage, Dr. Daniel Sigg, Dr. Paul Schwinberg, Richard McCarthy, Josh Myers, Joseph Betzweiser, for their generous advice and long experience; To David Levitan, Nicolas Smith, and Hunter Elliot, for their exceptional work and fellowship in the summer of 2005.

Competing Interests The authors declare that they have no competing financial interests.

Correspondence Correspondence and requests for materials should be addressed to Grant David Meadors (email: meadorsg@reed.edu) or H. Richard Gustafson (email: gustafso@ligo-wa.caltech.edu).